

Machine Learning Decoder for 5G NR PUCCH Format 0

Anil Kumar Yerrapragada*, Jeeva Keshav S[†], Ankit Gautam[‡], Radha Krishna Ganti[§]

Department of Electrical Engineering
Indian Institute of Technology Madras
Chennai, India 600036

Email: *anilkumar@5gtbiitm.in, [†]ee20d202@smail.iitm.ac.in, [‡]ee20m008@smail.iitm.ac.in, [§]rganti@ee.iitm.ac.in

Abstract—5G cellular systems depend on the timely exchange of feedback control information between the user equipment and the base station. Proper decoding of this control information is necessary to set up and sustain high throughput radio links. This paper makes the first attempt at using Machine Learning techniques to improve the decoding performance of the Physical Uplink Control Channel Format 0. We use fully connected neural networks to classify the received samples based on the uplink control information content embedded within them. The trained neural network, tested on real-time wireless captures, shows significant improvement in accuracy over conventional DFT-based decoders, even at low SNR. The obtained accuracy results also demonstrate conformance with 3GPP requirements.

I. INTRODUCTION

A wide range of wireless applications supported by 5G fall into three different use cases [1], [2]: Enhanced Mobile Broadband (eMBB), Ultra-Reliable Low Latency Communications (URLLC), and Massive Machine Type Communications (mMTC). To support these use cases, a fundamental building block of a 5G cellular system is the Physical Uplink Control Channel (PUCCH) that carries the Uplink Control Information (UCI). UCI is fed back from the User Equipment (UE) to the base station (gNodeB) and contains information such as (1) Hybrid Automatic Repeat Request (HARQ) Acknowledgements for prior downlink transmissions, (2) Scheduling Requests (SR) for uplink resources and, (3) Channel State Information (CSI) reports containing channel quality metrics that enable link adaptation and downlink resource allocation. Depending on the 5G use case, the UE can use one of five PUCCH formats [3]. Formats 0 and 1 can carry small UCI payloads (1 or 2 HARQ bits and an SR). Formats 2, 3, and 4 can transmit much larger payloads (HARQ, SR, and CSI reports). Formats 0 and 2 occupy two symbols in the time domain, making them ideal for low latency applications (URLLC). Formats 1, 3, and 5 can occupy up to 14 symbols, making them suitable for applications requiring enhanced capacity and coverage (eMBB and mMTC). We note that while the 5G standards [4]–[6] offer detailed descriptions of the transmitter steps for PUCCH signaling, the receiver implementation is largely left open.

Format 0 encodes the information in the phase of a waveform in the frequency domain. In this paper, we utilise a Machine Learning (ML) based receiver for the robust and accurate demodulation of UCI transmitted using PUCCH Format 0. We make the following contributions:

- We recast the problem as an ML classification problem. Then, taking inspiration from the success of neural networks in other domains, we apply similar approaches.
- We validate the trained neural network on test data obtained from MATLAB simulations. In addition, we test the network on real-time over-the-air data captured from a 3GPP compliant 5G testbed at IIT-Madras [7]. We also present comparisons with conventional Discrete Fourier Transform (DFT) based approaches.
- Applying ML models to solve wireless communications problems involves several key considerations such as realistic dataset generation, processing of complex numbers, and determining the optimum training SNR. As we describe our approach, throughout the paper we also provide insights into these considerations.

II. BACKGROUND ON PUCCH FORMAT 0

PUCCH Format 0 is used to transfer 1 or 2 HARQ acknowledgements and/or an SR [6]. Format 0 signalling does not contain any pilot reference signals (Demodulation Reference Signals (DMRS)) nor does it use Quadrature Amplitude Modulation (QAM) to modulate data. Instead, it transmits cyclically shifted versions of a pre-defined base sequence. The UCI is encoded in the cyclic shifts of a base waveform.

A. Format 0 Allocation and Sequence Generation

The cyclically shifted base sequence is then mapped to the Resource Grid where it occupies one Resource Block (RB) in the frequency domain and either one or two symbols in the time domain. Overall, either 12 or 24 Resource Elements can be occupied. The second symbol holds a sequence similar to that of the first symbol and can be used for enhancement of SNR at the receiver. The PUCCH Format 0 sequence in the frequency domain is given by,

$$r_{u,v}^{(\alpha,\delta)}(n) = e^{j\alpha n} \cdot \bar{r}_{u,v}(n) = e^{j\alpha n} \cdot e^{j\phi(n)\pi/4} \quad (1)$$

where $n = 0, 1, 2, \dots, N_{sc}^{RB} - 1$, where N_{sc}^{RB} denotes the number of subcarriers per resource block. The sequence, given by $\bar{r}_{u,v}$, is the low Peak-to-Average Power Ratio (PAPR) base sequence [4]. Lastly, $\phi(n)$ is given by Table 5.2.2.2-2 in [4]. The subscripts u and v represent the group number and the sequence number within the group respectively. They are determined by higher layer group hopping parameters. We note that when PUCCH Format 0 is two symbols long, intra slot frequency hopping can be enabled. In this paper, for ease of

exposition we assume intra slot frequency hopping is disabled. The cyclic shift applied to the base sequence is denoted by α and is given by,

$$\alpha = \frac{2\pi}{N_{sc}^{RB}} \left((m_0 + m_{cs} + n_{cs}(n_{s,f}^\mu, l + l')) \bmod N_{sc}^{RB} \right) \quad (2)$$

where,

- m_0 is the initial cyclic shift. Note that Fig. 1 is with respect to $m_0 = 0$. Other values of m_0 allow multiple users to be multiplexed on the same PUCCH Format 0 resources.
- m_{cs} is the UCI specific cyclic shift, shown in Fig. 1. One bit of HARQ can be transmitted using cyclic shifts 0 and 6. Two bits of HARQ and can be transmitted using cyclic shifts 0, 3, 6 or 9. A single SR bit can be transmitted with a single cyclic shift of 0. A combination of one bit of HARQ and an SR can be transmitted using cyclic shifts of 0, 3, 6 or 9. A combination of two bits of HARQ and an SR can be transmitted using cyclic shifts of 0, 1, 3, 4, 6, 7, 9 or 10.
- $n_{cs}(n_{s,f}^\mu, l + l')$ is a function based on the pseudo-random binary sequence defined in [4].
- $n_{s,f}^\mu$ is the slot number in the radio frame.
- l is the OFDM symbol number in the PUCCH transmission where $l = 0$ corresponds to the first OFDM symbol of the PUCCH transmission [4], [6].
- l' is the index of the OFDM symbol in the slot that corresponds to the first OFDM symbol of the PUCCH transmission in the slot [4], [6].

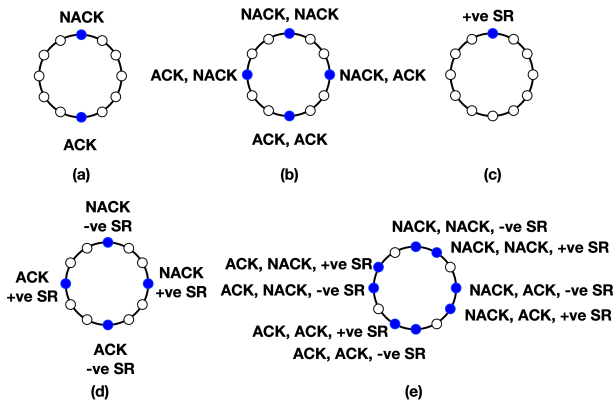


Fig. 1: The cyclic shifts m_{cs} applied to the PUCCH Format 0 base sequence depend on the specific UCI content.

B. Existing PUCCH Format 0 Receiver Methods

Decoding the UCI format 0 involves detecting the UCI specific cyclic shift m_{cs} applied to the base sequence by the UE. Format 0 decoding is different from other formats [8]. Since format 0 has no provision for DMRS, there is no channel estimation or equalization. Consequently, correlation based methods are used to decode the UCI.

The low PAPR base sequence is known at the receiver. The decoding method involves correlating the received samples with various cyclically shifted versions of the base sequence.

The applied cyclic shift is the cyclic shift that gives the highest correlation magnitude. The works in [9]–[11] provide a comparison of the correlation based receivers for various scenarios involving multiple antennas and multiple hops.

In this paper, we use the DFT based correlation for comparison. This method recovers the phase rotation α by taking the DFT of $e^{j\alpha n} \cdot \bar{r}_{u,v}(n) \cdot \bar{r}_{u,v}^*(n)$. The multiplication of the base sequence with its complex conjugate forces it to unity. The 12 point DFT then results in a peak at α . Recall from (2) that α is a combination of m_0 , m_{cs} and n_{cs} . Therefore, on subtraction of $m_0 + n_{cs}$ from α (subtraction is modulo 12), the UCI specific cyclic shift m_{cs} remains.

The DFT algorithm proves better from a hardware perspective due to its optimized use of resources (avoiding the need to correlate with all the shifted base sequences), reduced latency, and higher throughput. In the 5G testbed at IIT-Madras [7], a DFT based receiver for PUCCH Format 0 has been implemented on custom Field Programmable Gate Array (FPGA) boards.

III. ML BASED RECEIVER FOR PUCCH FORMAT 0

In this Section, we pose the detection of the cyclic shift m_{cs} as a machine learning classification problem. Classification is a supervised learning task that involves predicting a label given an input data instance. A classifier requires a training dataset, preferably with many instances of inputs and output labels from which to learn. A machine learning model such as a neural network can then look at the instances in the training dataset and learn the optimal mapping between input and output. It learns the mapping by minimizing a loss function. The loss function is some form of distance between the ground truth label and the label predicted by the neural network. ML models are attractive because they can replace manual feature extraction rules and the need to have an explicit mathematical function mapping the input to the output. A well-trained neural network can extract highly complex and non-linear features and mappings from a dataset that linear methods such as correlation may not capture. The capability of neural networks is evidenced by the fact that they have become adept at solving classification tasks across various domains, from computer vision to healthcare.

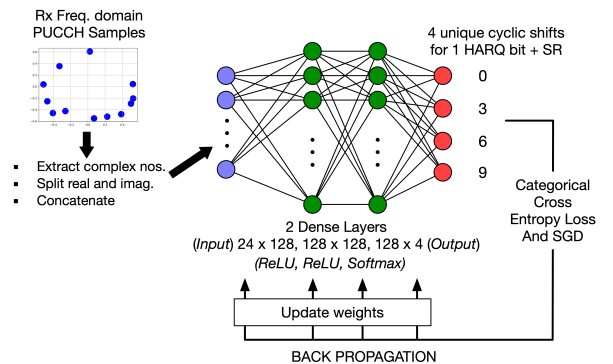


Fig. 2: PUCCH Format 0 decoder architecture.

A. PUCCH Format 0 detection as a classification problem

The classification task for the PUCCH Format 0 decoder is the following: Predict the applied cyclic shift m_{cs} based on the received Format 0 signal samples (in the frequency domain). The predicted m_{cs} in turn, maps to the UCI content (Fig. 1).

After the cyclic prefix removal and the FFT of the time domain waveform at the receiver, we extract the resource block containing the 12 PUCCH Format 0 samples. These samples serve as the input to the neural network, as shown in Fig. 2. The output labels are the applied cyclic shift m_{cs} , which have to be known for each input instance during training.

Note that the 12 resource block samples are complex numbers, leading to an key design issue. Commonly available neural networks and activation functions do not directly support complex number operations. Two options emerge. The first and most simple approach is to split each complex number into its real and imaginary components. Then either concatenate or interleave them to form one real vector of twice the size of the original complex vector. Another approach is to explore the notion of holomorphic neural networks and activation functions [12]. There is no proven theory that suggests that one method is better than the other. This paper chooses to adopt the first approach due to the ease of neural network implementation. Building real-valued neural networks is straightforward using commonly available Machine Learning libraries such as Tensorflow and PyTorch.

B. Dataset generation

Dataset generation in ML for communication has a unique set of challenges. Firstly, benchmark datasets are not as widely available as in the image classification domain. Secondly, when seeking a model that one can deploy in a real-world system, it is desirable to use signal datasets captured from the actual hardware. Developing such datasets requires access to communication system hardware or testbeds. In the absence of such hardware, several state-of-the-art simulation tools such as the MATLAB 5G Toolbox exist to generate near-accurate datasets under various channel impairments. Furthermore, it is less tedious to create and pre-process large datasets using simulation tools than on hardware testbeds. Simulated data is a good starting point for training neural networks in communication problems. Hardware data, if available, can then be used to validate the performance in real world scenarios. For this paper, we use a combination of the two approaches.

1) *Simulated data for training:* Using the MATLAB 5G Toolbox, we generate received waveforms containing the PUCCH Format 0 signals. These waveforms include fading channel impairments and Additive White Gaussian Noise (AWGN). For various SNR values (0, 5, 10, 15, and 20dB), we generate PUCCH signals transmitted over a TDL-C Channel and store the noisy received samples. These samples are the input data. For each input, the corresponding output label is the applied cyclic shift m_{cs} .

2) *Hardware captures for testing:* We use hardware captures derived from our state-of-the-art 5G testbed at IIT Madras [7] for more realistic testing. The setup (see Fig. 3) consists of an N5182B Vector Signal Generator (VSG) for transmitting the 5G signal at a center frequency of 3.49986

GHz (sub-6 GHz raster in the n78 band). The antenna used is a commercial omnidirectional wideband monopole. The antenna transmits signals originating from a Vector Signal Generator (VSG). The VSG is connected to the antenna through 2 SMA cables with 1.9 dB wire loss each.

A multi-channel receiver front end connected to a dual-polarized antenna receives the signals from over the air (For the purpose of the paper, we utilise only one antenna and one-transceiver chain). Other receiver components include an in-house Low Noise Amplifier (LNA) with 60dB gain at the receiver front end and an ADRV 9009 RF transceiver. We place the transmitter one meter away from the receiver to emulate a real-time wireless scenario. The PUCCH Format 0 signal is transmitted from the VSG through an antenna, in the air, then received at the LNA, followed by the transceiver. The signal out of the 16-bit ADC is then collected and used for testing.



Fig. 3: IIT-Madras 5G testbed setup with the Remote Radio Head used as a receiver and the VSG used as a transmitter.

In both the software and hardware datasets, without loss of generality, we focus on the case where the UCI contains one HARQ bit and an SR. We generate 200000 instances for various SNR values. In each instance, the transmission includes a randomly chosen combination of 1 HARQ and SR bits and the corresponding cyclic shift m_{cs} is applied to the base sequence. Our experiments revealed that the function n_{cs} in (2), which varies with slot and symbol index, is one of the characteristics of the data that neural network latched onto. Further, we conjecture that the neural network might be affected by change in the initial cyclic shift m_0 as well. Since incorporating all combinations of n_{cs} and m_0 into the training process is time prohibitive, in this paper we constrain ourselves to the most commonly scheduled scenario by layer 2

in our testbed i.e., data with a single m_0 of 0 and two different slots (13 and 14) in the frame.

C. Neural Network Architecture

There is no get-rich-quickly approach to determining the optimum neural network architecture. In the absence of such a formula, we have performed several experiments. Fig. 2 shows one of the architectures that showed the best performance during training and testing. All performance curves in this paper are with respect to this configuration. Fig. 7 compares all architectures that were tested.

1) *Structure of the neural network:* We employ a fully connected neural network with an input layer size of 24 neurons. The 24 corresponds to the concatenated real and imaginary parts of the 12 format 0 samples. The two intermediate layers are dense layers containing 128 neurons each. And the output neurons each represent one of four classes.

2) *Regularization:* To prevent overfitting, we apply dropout between all the layers, with a probability of 0.5. Dropout [13] is a regularization [14] technique that acts as a shortcut to achieve training the same model in multiple configurations of connections. It does so by randomly dropping some neurons during the training phase. A common cause for overfitting is neurons in subsequent layers compensating for "mistakes" made by those in prior layers. Dropout prevents this from happening, thus making training more noisy yet more robust at the same time.

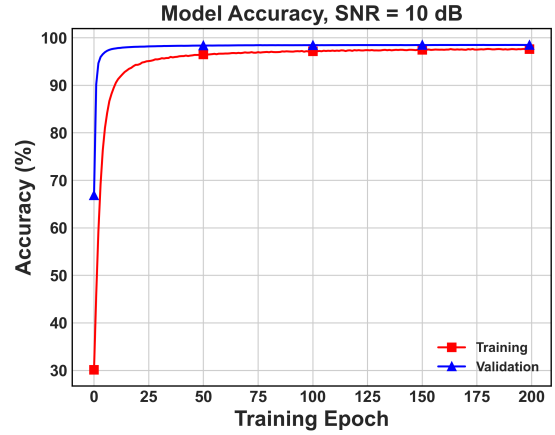
3) *Activations and Backpropagation:* Lastly, we add non-linearity to the neural network through Rectified Linear Unit (ReLU) activation functions in the dense layers. Since we require probabilities of each class at the final layer, we use the softmax activation function. Stochastic Gradient Descent (SGD) on the Categorical Cross-Entropy loss function makes up the backpropagation. In order to speed up learning while using SGD, we apply momentum which maintains an exponentially decaying moving average of prior gradients and moves in their direction [14].

D. Training and Testing

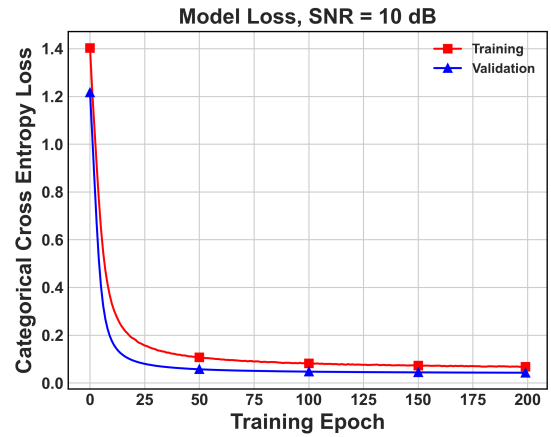
The choice of training SNR is far from trivial [15]. Low SNRs obscure features of the data while high SNRs impede generalization against channel impairments. An impractical but straightforward approach would be to divide the data into SNR buckets and train a separate neural network for each bucket. However, ideally, one would like a single trained neural network to work over a wide range of SNRs. To this end, we train the neural network on 200000 data samples generated in MATLAB at a middle SNR of 10 dB. Note that we use 75% of the dataset for training and the remaining for testing. We then test this neural network on simulated datasets of all 5 SNRs (0, 5, 10, 15, and 20dB). Finally, we also use the same trained neural network to test with actual wireless hardware data captured using the IIT-Madras 5G testbed. We have settled on a training duration of 200 epochs through experiments.

IV. RESULTS AND DISCUSSION

In this Section, we describe the results obtained from training and testing the neural network in various configurations.



(a)



(b)

Fig. 4: (a) Training Accuracy and (b) Loss of the Neural Network. Simulated data at an SNR of 10dB is used for training.

Prior work adopts two types of performance metrics [9]–[11] - False detection and Missed Detection. False detection refers to the gNB receiver predicting that UCI was sent when in fact nothing was sent. Missed detection refers to the gNB receiver not identifying a true UCI transmission by the UE. In this paper we adopt a slightly different metric (that also encapsulates missed detections), leaving false detection for immediate future work.

In keeping with other Machine Learning papers, we use accuracy as an evaluation metric. Accuracy is the ratio of correct predictions to the total number of predictions. It is the probability that the neural network believes a specific type of UCI was sent, given that some UCI was indeed sent by the UE. Furthermore, the accuracy metric by definition, incorporates the inverse of missed detections - correct decoding of UCI inherently means that the gNB has not missed the detection. False detections can easily be incorporated into our framework by adding an additional label class whose inputs would be instances of AWGN.

Fig. 4 shows the training and validation accuracy and loss. A generally increasing accuracy and decreasing loss, ultimately leading to convergence is indicative of a neural network that has learnt well. Furthermore, validation accuracy/loss values are slightly better, but not too much better than the training values suggesting that the neural network has not overfit. It also suggests that new unseen data has sufficient variance and is not skewed in favor of any one class.

Test Accuracy as a function of SNR is shown in Fig 5¹. There is an increase in accuracy with SNR with simulated test data, as expected. The neural network shows a clear gain versus the DFT algorithm. Hardware test data follows a similar trend. Both simulations and hardware captures show accuracy values greater than 99% for a wide range of SNR, thus surpassing the 3GPP conformance requirements [16].

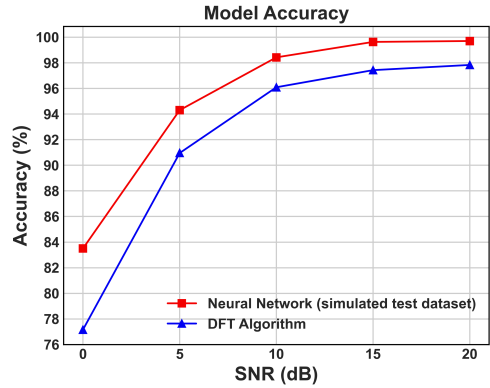
A significant gain in accuracy with the neural network is seen at the very low SNR end of the curves in Fig. 5. We observe about $3dB$ gain in performance of the neural network compared to the DFT method for simulated data. At higher SNRs, both methods seem to converge. This is more evident when the neural network is tested with the actual hardware samples. This might be because:

- 1) As a result of the complex nature of setting up and operating hardware testbeds, there is currently a discrepancy in the sizes of the simulated and hardware datasets. At this time, the transfer of many hardware captures to the host computer is limited by the throughput of the Joint Test Action Group (JTAG) standard. Over time, we expect this to improve by adopting other methods.
- 2) The training data set (generated using MATLAB), might not incorporate all the non-idealities that are seen in real hardware.

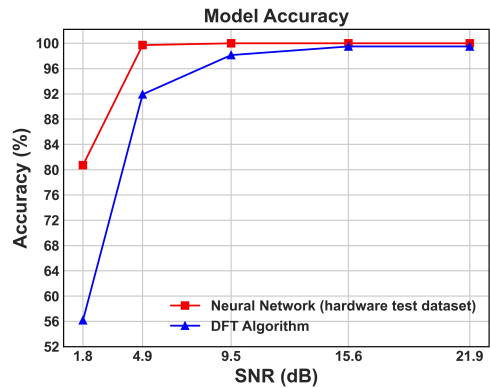
A confusion matrix is often used to measure the performance of a classification model. This offers a different perspective from accuracy and loss in that it indicates the true and false positives in the prediction, i.e., the number of times each class was predicted correctly versus incorrectly. The confusion matrices for the neural network tested with both the simulated and hardware datasets are shown in Fig. 6. It can be seen that the maximum values lie along the diagonal and are much larger than the off diagonal elements. This shows that the majority of the predictions made by the neural network are correct.

With the aim of making the neural network hardware-worthy, in this paper we begin an analysis on the impact of neural network size. Fig. 7 shows the test accuracy versus SNR for various configurations of the neural network. These experiments are performed on simulated test datasets. While in this paper, we have provided the results with a neural network with 2 layers and 128 neurons in each layer, we observe that similar performance can be obtained using 2 layers and 32 neurons in each layer, thereby significantly cutting the complexity of the network. However, we note that more specific analysis with specific hardware devices and hardware captured datasets is necessary.

¹For SNR in Fig 5a, signal power is calculated considering the entire time domain received waveform for 1 slot. For SNR in Fig 5b, signal power is calculated by extracting the PUCCH location from the received spectrum.



(a)



(b)

Fig. 5: Model accuracy on (a) simulated test data, (b) hardware captured test data. In both cases the testing accuracy is compared with that achieved by the DFT based decoder.

V. CONCLUSION AND FURTHER WORK

In this paper, we have evaluated the performance of a neural network classifier in its ability to decode Uplink Control Information transmitted on the PUCCH using format 0. Results show improvements in detection capabilities compared to mathematical approaches such as the DFT. Future work must investigate the feasibility of data generation and neural network training for all possible values of m_0 , m_{cs} and n_{cs} . Secondly, an extended classifier could include an additional class for detecting the scenario when nothing is transmitted (false detection classification). Lastly, to aid the real-time deployment of the trained neural network, it would be prudent to analyze its complexity from a hardware chip implementation perspective.

ACKNOWLEDGMENT

The authors would like to thank the Department of Telecommunications (DOT), India for funding the 5G Testbed project and the Ministry of Electronics and Information Technology (MeitY) for funding this work through the project "Next Generation Wireless Research and Standardization on 5G and Beyond".

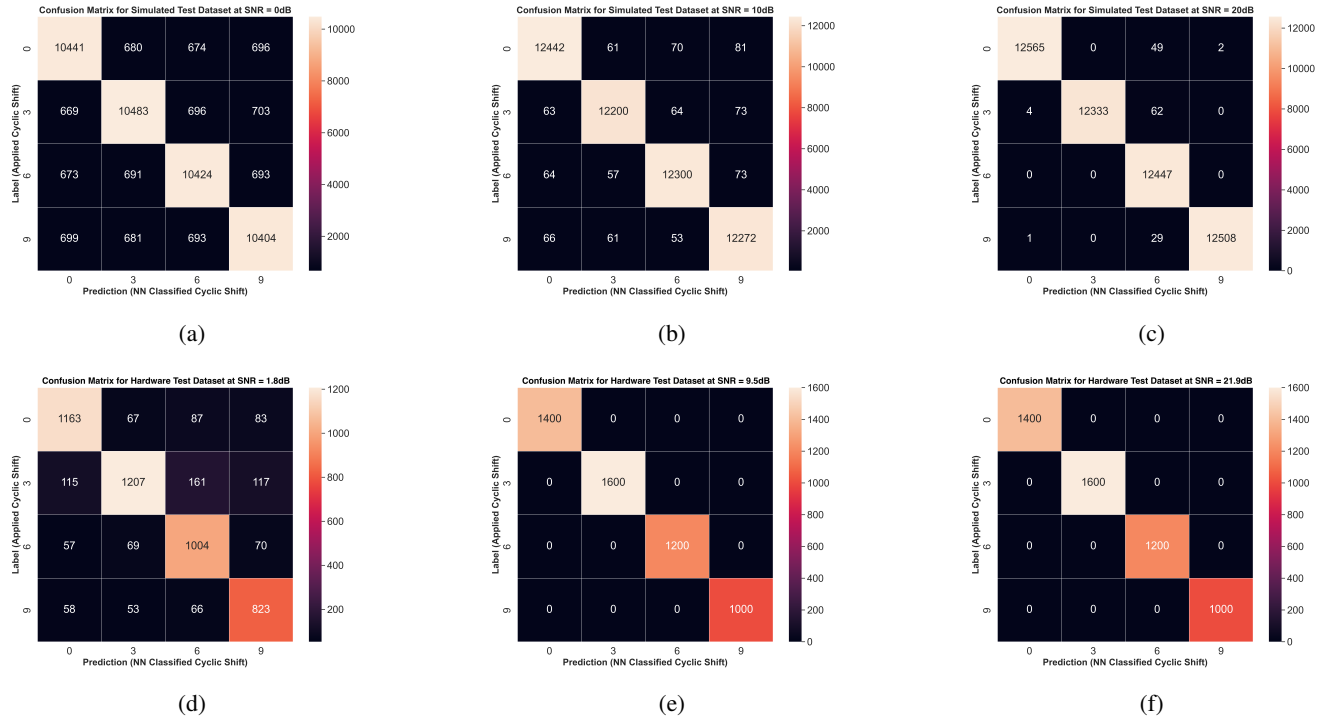


Fig. 6: Confusion Matrices for MATLAB simulated test data at (a) SNR = 0 dB (b) 10 dB (c) 20 dB. Confusion Matrices for hardware captured test data at (d) SNR = 1.8 dB (e) 9.5 dB (f) 21.9 dB

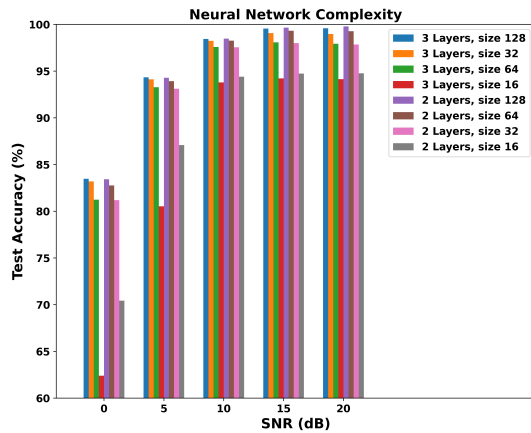


Fig. 7: Neural network performance for various configurations of complexity.

REFERENCES

- [1] P. Nikolich, C. Lin, J. Korhonen, R. Marks, B. Tye, G. Li, J. Ni, and S. Zhang, "Standards for 5G and beyond: Their use cases and applications," *IEEE 5G Tech Focus*, vol. 1, no. 2, 2017.
- [2] P. Popovski, K. F. Trillingsgaard, O. Simeone, and G. Durisi, "5G wireless network slicing for eMBB, URLLC, and mMTC: A communication-theoretic view," *IEEE Access*, vol. 6, pp. 55 765–55 779, 2018.
- [3] C. Johnson, *5G New Radio in Bullets*, 1st ed. Farnham, England: Self-Published, 2019.
- [4] 3GPP, "Physical Channels and Modulation," 3rd Generation Partnership Project (3GPP), Technical Specification (TS) 38.211, 2021, version 16.5.0.
- [5] 3GPP, "Multiplexing and Channel Coding," 3rd Generation Partnership Project (3GPP), Technical Specification (TS) 38.212, 2021, version 16.5.0.
- [6] 3GPP, "Physical Layer Procedures for Control," 3rd Generation Partnership Project (3GPP), Technical Specification (TS) 38.213, 2021, version 16.5.0.
- [7] "5G Testbed IIT Madras," <http://www.5gtbitm.in/>, 2020, [Online; accessed 25-Aug-2022].
- [8] L. Kundu, G. Xiong, and J. Cho, "Physical uplink control channel design for 5G new radio," in *2018 IEEE 5G World Forum (5GWF)*. IEEE, 2018, pp. 233–238.
- [9] Y.-H. Kim, H. Ju, C. B. Jeong, and M.-S. Lee, "Performance comparison of DTX detection schemes for 5G NR PUCCH," in *2020 International Conference on Information and Communication Technology Convergence (ICTC)*. IEEE, 2020, pp. 1391–1394.
- [10] D.-M. Phan and P. N. TH, "An Enhanced Method to Improve Signal Reception Performance for 5G NR Physical Uplink Control Channel with Frequency Hopping Configuration," in *2021 International Conference on Advanced Technologies for Communications (ATC)*. IEEE, 2021, pp. 13–17.
- [11] S. Tadavarty and N. K. Chavali, "Performance Analysis of 5G NR PUCCH Format 0 Receiver," in *2021 IEEE 18th India Council International Conference (INDICON)*. IEEE, 2021, pp. 1–5.
- [12] J. Bassey, L. Qian, and X. Li, "A survey of complex-valued neural networks," *arXiv preprint arXiv:2101.12249*, 2021.
- [13] N. Srivastava, G. Hinton, A. Krizhevsky, I. Sutskever, and R. Salakhutdinov, "Dropout: A simple way to prevent neural networks from overfitting," *The journal of machine learning research*, vol. 15, no. 1, pp. 1929–1958, 2014.
- [14] I. Goodfellow, Y. Bengio, and A. Courville, *Deep Learning*. MIT Press, 2016, <http://www.deeplearningbook.org>.
- [15] T. O'shea and J. Hoydis, "An introduction to deep learning for the physical layer," *IEEE Transactions on Cognitive Communications and Networking*, vol. 3, no. 4, pp. 563–575, 2017.
- [16] 3GPP, "Base Station (BS) conformance testing. Part 1: Conducted conformance testing," 3rd Generation Partnership Project (3GPP), Technical Specification (TS) 38.141, 2021, version 16.6.0.